FATIGUE LIFE ANALYSIS OF HYBRID E-GLASS/CARBON FIBRE POWDER EPOXY MATERIALS FOR WIND TURBINE BLADES

Evanthia J. Pappa[1], James J. Murray[1], Michael Walls[2], Parvez Alam[1], Tomas Flanagan[2], Adrian Doyle[2], Sandro Di Noi[3], Edward D. McCarthy[1], and Conchur M. Ó Brádaigh[1]

[1] School of Engineering, Institute for Materials and Processes, University of Edinburgh, Edinburgh EH9 3FB, Scotland, UK
Email:e.pappa@ed.ac.uk, Web Page: www.eng.ed.ac.uk
[2]ÉireComposites Teo, An Choill Rua, Indreabhán Co. Galway H91Y923 Ireland
Email: a.doyle@eirecomposites.com, Web Page: www.eirecomposites.com
[3]SE Blades Technology B.V. Jan Tinbergenstraat 290, 7559 ST Hengelo (Overijssel), The Netherlands
Email: S.Di.Noi@suzlon.com, Web Page: www.suzlon.nl

Keywords: Wind turbine blade, demonstrators, hybrid composites, fatigue analysis, renewable energy

Abstract
A medium scale demonstrator of a hybrid glass/carbon fibre composite wind turbine blade spar cap/root joint was designed, manufactured and tested statically and dynamically. The current study describes a the step-wise pattern of the demonstrator, its manufacturing and mechanical testing. The glass-carbon fibre transition and ply drop-off strengths are critical to the design of the blade. The design of the glass-carbon transition demonstrator aims to provide a constant stiffness over the specimen length whilst concurrently aiming to keep stress concentrations at a minimum. The specific composite structure combines triaxial and biaxial E-glass and carbon fibres embedded in a powder epoxy matrix. One of the most important aspects of this work relates to the damage response of the coupons. The fatigue analysis of the coupons and the failure mechanisms, such as interfacial delamination and debonding within the transition are presented for all examined coupons. The results provide sufficient evidence to describe the mechanical behavior of the demonstrator over time, and they indicate that the demonstrator has structural integrity over a fatigue life of >1M cycles at 50% of the ultimate tensile strength.

1. Introduction

According to WindEurope, the former European Wind Energy Association (EWEA), the offshore wind sector in Europe generated a record of 3148 MW of net additional installed capacity in 2017; 53% of which was generated by the UK[1]. In recent years, both blade sizes and the commercial production volumes of wind blades have significantly increased (approx. 23% per annum [1]); thus, advanced materials and improved designs are required [2, 3]. As the length of the blades increases, the specific strength and stiffness also need to increase. High specific stiffness, good fatigue properties, low densities and the easy tailorability of fibre reinforced polymers (FRP) make them ideal materials for longer blade designs. Although carbon fibre (CF) is stronger, more fatigue-resistant and less dense than E-glass, its high cost remains problematic for the commercialisation of wind turbine blades [4-6, 8]. This is especially evident where thick FRP sections are required [7, 9]. However, the arrival of new materials, such as high performance carbon fibres with improved sizings and specifically formulated powder epoxies [11-13] are interesting for the design of superior quality blades with cost-effective manufacturing processes [4]. Vacuum infusion processing (VIP) and vacuum bag only (VBO) are processing techniques commonly used for the manufacture of wind turbine blades. VBO is of particular importance to emerging industries such as marine renewable energy (MRE), as is the most cost effective manufacturing method. Nevertheless, thick-section processing requires a low cure

exotherm, a short infusion time window and rapid cure response so that the process cycle time can be reduced without compromising the quality of the part [14-19]. Maguire et al., studied a cost- effective model for the process cycle time of the curing process and proved that a thick-section part could be fully or partially consolidated in one stage and then assembled and fused together in a separate stage to produce "one-shot" cured parts, without a further adhesive bonding stage [14, 27]. This project introduce a thickness-tapering design using an epoxy powder resin where the parts were initially consolidated and then assembled together for a "one-shot" cure process.

To improve the reproducibility and decrease high scatter in measured mechanical properties, optimised designs are needed. In this study, thickness-tapering was employed to tailor the specific stiffness and specific strength of thin-walled structural elements subjected to spatially distributed loads. The tapering was introduced by terminating plies at different locations, also known as ply drop-offs. Ply drop-offs cause discontinuities within a laminate and therefore introduce structural complications, such as stress concentrations and through-thickness stresses, leading to potential failure of the components through delamination and/or failure of the resin. Stress concentrations at ply drop-offs can lead to premature failure at loads well below the material's inherent strength. As a consequence, the advantages of introducing ply drops may be outweighed by the disadvantages. The stress-raising effects of ply drop-offs depend on several design variables. These include the orientation and position of the terminated plies within the laminate, the overall laminate stacking sequence and the nature of the applied load. In this project, the design of the glass-carbon transition demonstrator aimed to provide a constant stiffness over the length of the specimen whilst concurrently aiming to keep stress concentrations at a minimum.

A rotor operates under random loads, and wind turbine blades experience a large number of fatigue cycles throughout their service life, approx. 10^{8-9} [25, 28]. When a blade is in the horizontal position, the blade's mass generates cyclic stresses with a maximum load near the leading and trailing edges. In addition, there is a) wind shear loading when both blades are vertical and the flapwise load is lower at the vertically downward position than that at the vertically upward position due to the vertical wind shear profile, and b) gravitational loading on the blades throughout the blades' rotation cycle [5, 9, 10, 20-25]. In this project, the tapering demonstrator is representative of many features in the spar cap of a wind turbine blade. The stress concentrations at the ply drop-offs can cause premature failure of blades in either static or dynamic loading and so it is important to test the demonstrators in both static tension and in fatigue. The fatigue life of such a structure is heavily dependent on regions of stress concentration. Micro-cracking in such regions can lead to the catastrophic failure of the entire structure in a relatively short number of cycles. As such, it is important to design so that stresses remain well below the endurance limits of the material. In the following sections, preliminary fatigue results for the ply-drop off of a glass-carbon transition demonstrator are presented. In section 2.1, the design of the demonstrator is described, followed by the materials used and the manufacturing process in section 2.2. Furthermore, section 2.3 provides preliminary fatigue test results with a discussion on the failure mechanisms of the demonstrator specimens. Finally, conclusions and suggestions for future work are discussed in section 3.

2. Experimental

2.1. Design

The design of the glass-carbon transition demonstrator aimed to provide a constant stiffness over the length of the specimen in order to keep stress concentrations to a minimum. To achieve this, the proposed design consisted of a scarf joint and a back-to-back configuration (Fig. 1). The stacking sequence of the plies was balanced and symmetric with respect to the laminate midplane. In addition to the slope of the ply drop-off regions, their location in a stack is also important, therefore, a step-wise pattern was incorporated into the design. This step- wise pattern of ply drops was preferred since at the start and the finish of the ply drop regions, the dropped plies are centred in the mid plane. To

avoid abrupt ply terminations, the ply drop-off did not exceed a distance of 0.20mm per drop. The dropped plies were evenly distributed through the laminate thickness. The width of each specimen was 35mm with a clamping length of 110mm (for subsequent mechanical testing).

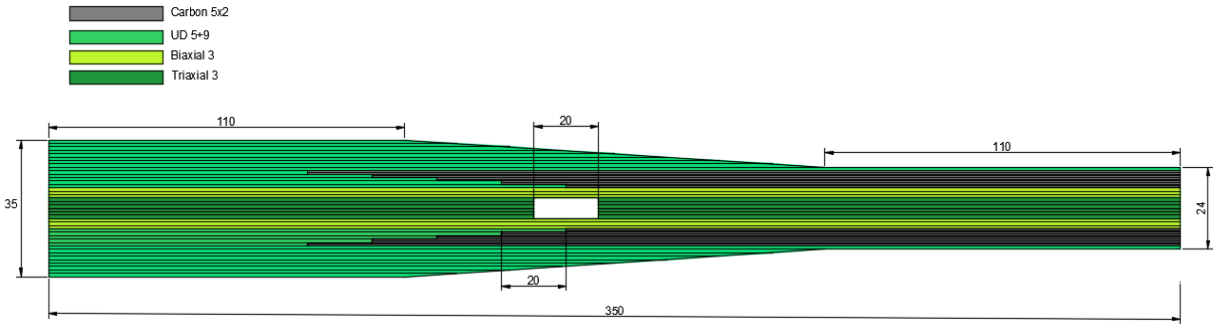

Figure 1. The design of the glass-carbon transition demonstrator is a back-to-back configuration with a hollow-out in the middle section.

The demonstrator component was made of two similar pieces which were bonded in a back-to-back configuration. This configuration of the test elements was manufactured by first curing each side and then bonding the two parts together; more details are provided in section 2.2.

2.2. Materials and Methods

Commercially available continuous tow carbon fibres T700S-24K-50C (1% sizing agent) from TORAYCA® (Toray Industries, Inc.) were used. The uni-directional (UD) E- glass, Triaxial E-glass fibre 1200g/m^2 and Biaxial E-glass fibre 600g/m^2 supplied by P-D Glasseiden GmbH Oschatz, Hexcel Reinforcements UK Limited and Cristex UK respectively. The powder epoxy resin used for the manufacturing of the demonstrators was EC-CEP-0016, supplied by EireComposites Teo. with a density of 1.22 kg/cm^3. The processing of this powder epoxy was characterised by Maguire et al. [14], while the compatibility of the carbon fibre sizing with the powder epoxy was studied by Mamalis et al.[11]. As the thickness of carbon fibre (CF) layers used was smaller than that of the unidirectional (UD) E-glass, two layers of CF were used for each layer of E-glass. Once the fabrics were cut to the correct size, and the amount of powder required for each layer was applied, the composite was then laid up. A stainless steel caul plate was used on one side to create a flat surface and a polyimide release film was laid on the uneven bagged surface. To ensure that the layers were correctly aligned, one side of the laminates was taken as a reference and each subsequent layer was aligned with this edge. This was especially important for laying up the stepped layers as there was a higher risk of misalignment. The alignment was also checked along the edge of the demonstrator to minimise the risk of misaligned fibres. The completed demonstrator was covered with release film and vacuum bagged. The curing cycle consisted of a B-stage cure, as described in [24].

After curing, the panel was machined according to the design in section 2.1. The scarf joint is formed from a ply drop that narrows as a function of distance along the joint. Underlying the transition between the GFRP and CFRP segments was a hollowed out region surrounded by two GFRP segments. The purpose for this hollow section in demonstrator design was to guide failure to the centre of the demonstrator. The gap/slot in each specimen was approx. 2.5mm deep and 20mm in length. Due to slot machining requirements, the pieces were bonded with a structural adhesive, Loctite EA 9394 QT AERO paste, in a back-to-back configuration as shown in Figure 2. Note that in wind blade manufacturing, no adhesive would be used; both components would be co-cured in a “one-shot” cure process.

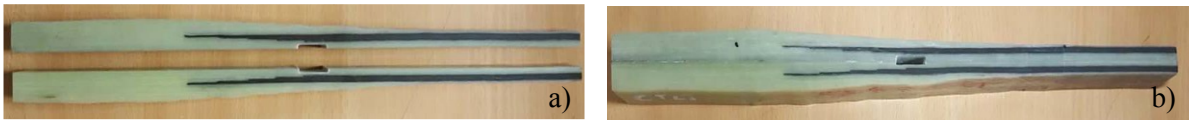

Figure 2. The bonding process of the two specimens (a) and the back-to-back configuration as one coupon (b).

After bonding, the demonstrators were cleaned, deburred and prepared for testing. The environmental conditions for both dynamic and static tests were: room temperature at approximately 20ºC and a relative humidity level of 53%. For the static test a gripping pressure of 100 bar was operated, while for the dynamic testing, all specimens were cyclically loaded in tension-tension (R=0.1) at 3Hz using a gripping pressure from (50-80) bar at either 40%, 50%, 55%, 60%, 65%, 70% and 75% of the estimated static failure load. The results are presented and discussed in the following section 2.3.

2.3 Results and discussion

During their operational life, wind turbine blades experience aerodynamic, gravitational and centrifugal forces. However, it is not always practical to determine combined load cases over critical cases, so in this work only critical cases are considered. The expected life span of wind turbine blades is approximately 20 years so they must be able to withstand *ca*. 2 x 10^8 load cycles. Due to the large variations in stress across the length and thickness of the demonstrator, it is the practice to determine an endurance load limit as opposed to an endurance stress limit. In this study, a total of 44 test demonstrators were manufactured and tested to determine both static tensile and fatigue properties. An average failure load of 261kN (SD= 23.2kN) was extracted from the later static tests, see Table 1.

Table 1. Static test results of the demonstrators.

Specimen No.	*Ext. at failure (mm)*	*Failure Load (kN)*
1	2.62	252.8
2	3.67	285.9
3	3.79	270.9
4	3.00	254.9
5	3.59	265.4
6	5.83	293.4
7	3.46	219.5
8	2.60	248.2
Average	***3.57***	***261.4***
SD	***1.03***	***23.2***
CoV (%)	***28.9***	***8.9***

The estimated failure load had been defined as 245kN based on earlier assumptions, therefore all the dynamic tests were carried out with the estimated failure load. According to the results (Table 2 and Figure 3), neither the specimens at 40% or 50% load had failed by 1,000,000 cycles and testing was discontinued, while the specimens at the rest of the loads resulted failed. In Figure 3, a linear trend for the failed specimens is derived.

Table 2. Dynamic test results of the demonstrators.

% F_{max}	*Load (kN)*	*No. of cycles to failure*
40	98.0	1,000,000 (stopped)
50	122.5	1,000,000 (stopped)
55	134.7	148,532
60	147.0	114,541
65	159.2	18,141
70	171.2	17,335
75	183.7	10,505

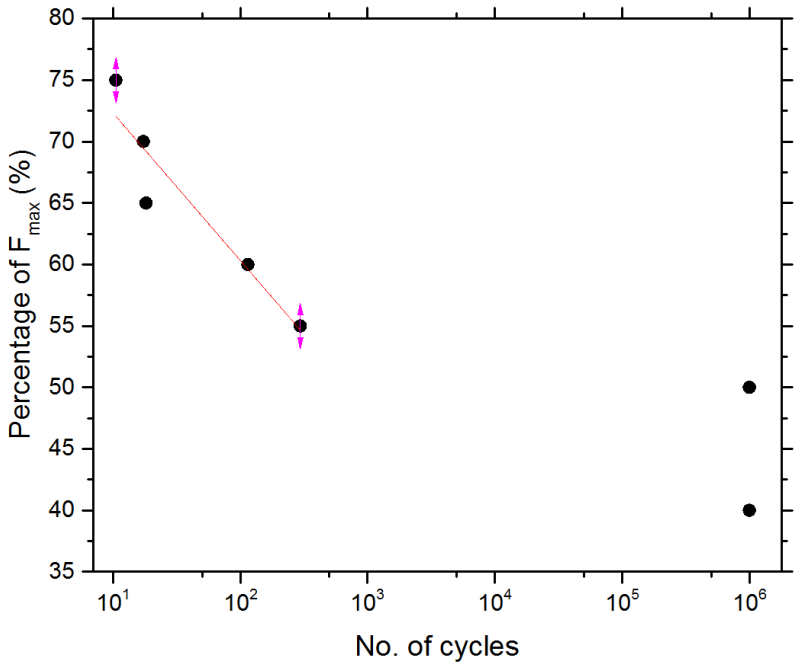

Figure 3. Fatigue test results for all cases. A linear trend for the fractured specimens is depicted.

Alam et al. [26] investigated the mechanical properties of CFRPs embedded in powder epoxy resins under cyclic load, where they were reported to fracture in an explosive manner. This style of failure was also observed to occur to some extent in the demonstrators. More precisely, failure was catastrophic in all cases with debonding in the transition between the GFRP and CFRP, interfacial delamination in both the GFRP and CFRP, fibre breakage, and matrix cracking, as shown in Figure 4. Contrary to the work in [26] no cross (perpendicular fibre) failures were observed. Rather, the failure in the demonstrators was dominated by shearing at interfaces, which from video footage, was noted to instigate from the hollowed-out section. This is evident in Figure 4, where fractures are preponderant in the loading axis of the demonstrator. Since failure is initiated at the hollowed-out section, debonding between the CFRP and the GFRP presumably follows the same step-wise path of the ply-drops. This is evidenced in Figure 5 where holes are visible at the ply-drops (in red boxes). The ply drops therefore serve to temporarily stunt the propagation of the debonding in the transition zone by absorbing some of the fracture energy.

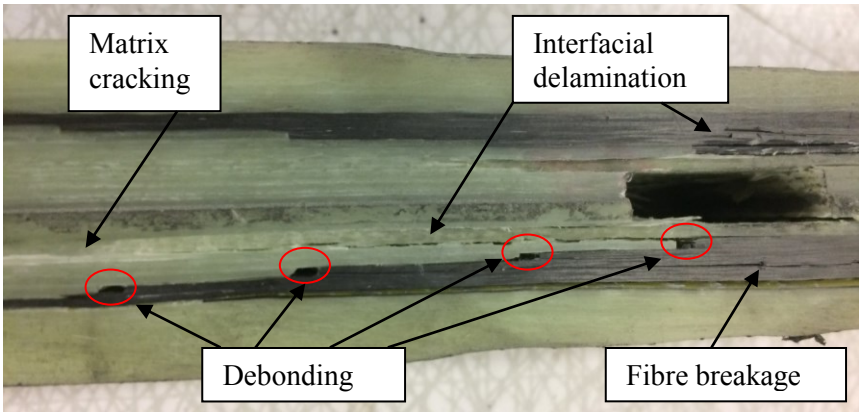

Figure 4. Failure mechanisms in demonstrator coupon including fibre breakage, debonding in the transition at the ply drop-offs, matrix cracking and interfacial delamination.

Nevertheless, the ply-drops also fail at the glass-carbon transition zone, transverse to the loading direction, and to the direction of the propagating debond. The transverse tensile debond is considerably weaker than debonding through shear and as such, even though the ply-drop serves to retard some fracture energy, it also acts as a point of weakness that leads to a transverse opening. Designing the most effective ply-drops is therefore of paramount importance as if they are sufficiently large, they will be more effective at blunting cracks within the demonstrators. However, being large is also a drawback, as if large ply-drops do themselves debond in a transverse to loading direction, they leave the demonstrator considerably weaker and disrupt the solid state continuum that would otherwise hold and transfer load.

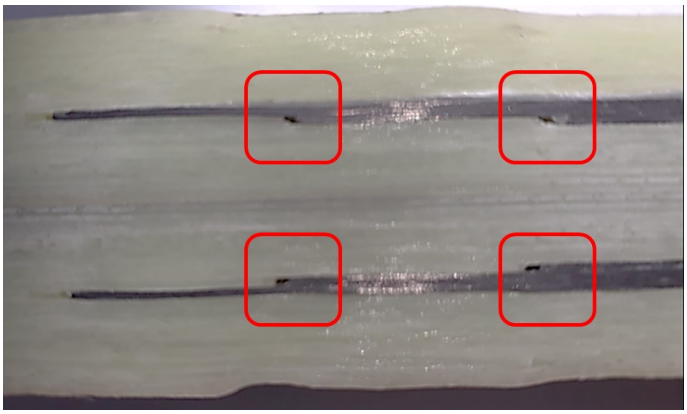

Figure 5. Highlighting the redirecting of fracture at the ply-drops.

The ply drop demonstrator, described in this study, is an example of a structure which features many of the design aspects and challenges of current composite ply-drop technology. These include the characteristics of the novel powder-epoxies being investigated, as well as structural features (e.g. ply drops) associated with turbine blade design. Power epoxy hybrid composites can have a significant positive impact on reducing the cost of manufacture of durable structures for the renewable energy industries, since all the parts of a wind turbine rotor can be assembled without adhesive bonding. In this project, a medium-scale tapered demonstrator was designed, manufactured and tested under cyclic load to determine its life cycle. Normally, ply drop-offs would create structural anomalies such as stress concentrations at the drop-location that could to a decrease the stiffness and strength of a blade. However, the introduction of a glass-carbon transition reduces the severity of this effect to a minimum in a cost-effective manner.

3. Conclusions

In this study, debonding in the interface between the GFRP and the CFRP region was detected in all demonstrator specimens. In addition, interfacial delamination was also detected, which was more severe for the GFRP sections than for the CFRP sections. In the middle section of each demonstrator, a slot was introduced to guide the failure at that point. In most cases, failure occurred as a consequence of debonding in the interface which was close to the middle section. That debonding decreased the strength of the coupon in the middle section which then caused catastrophic matrix cracking. Overall, it is clear that if the CFRP insert is not used to its full capacity, the endurance limit of the demonstrator will be reduced from its potential endurance limit. From this, we are able to conclude that in any further work, demonstrators should be designed to circumvent interfacial failure between the CFRP and the GFRP, so as to ensure that the CFRP insert is used to its fullest extent. Future studies involve new designs of drop-off and "one shot" cure process for the whole coupon.

Acknowledgments

The authors gratefully acknowledge financial support from MARINCOMP, Novel Composite Materials & Processes for Marine Renewable Energy, a Marie Curie FP7 Project funded under the IAPP call (Grant No. 612531), the Institute of Materials and Processes at the University of Edinburgh, industrial partners SE Blades Technology B.V. and ÉireComposites Teo. We would also like to acknowledge the technical support of the Materials Laboratory at the University of Aberdeen, the National University of Ireland Galway (NUIG) and University College Dublin (UCD).

References

[1] WindEurope. Offshore Wind in Europe: Key trends and statistics 2017. *WindEurope Annual Statistics Report*: windeurope.org, 2017.

[2] P. Purnell, J. Cain, P. Van Itterbeeck and J. Lesko. Service life modelling of fibre composites: A unified approach. *Journal of Composites Science and Technology,* 68:3330-3336, 2008.

[3] P. Jamieson. *Innovation in wind turbine design*. John Wiley & Sons Ltd, 2018.

[4] T. Flanagan, J. Maguire, C.M. Ó Brádaigh, P. Mayorga, and A. Doyle. Smart Affordable Composite Blades for Tidal Energy. *Proceedings of the 11th European Wave and Tidal Energy Conference, Nantes, France,* September 6-11 2015.

[5] J. Hayton. *Offshore wind farms: Technologies, design and operation.* Elsevier. 2016.

[6] T. Hoang, L. Queval, L. Vido and C. Berriaud. Impact of the rotor blade technology on the levelized cost energy of an offshore wind turbine. *Proceedings of the International Conference on Optimization of Electrical and Electronic Equipment (OPTIM), Brasov, Romania,* May 25-7 2017.

[7] P. Davies and Y. D. S. Rajapakse. *Durability of composites in marine environment 2*. Springer. 2018.

[8] P. Brøndsted, H. Lilholt and A. Lystrup. Composite materials for wind power turbine blades. *Annual Review on Materials Research,* 35:505-538, 2005.

[9] Y. S. Song, J. R. Youn and T. G. Gutowski. Life cycle energy analysis of fiber- reinforced composites. *Journal of Composites; Part A,* 40:1257-1265, 2009.

[10] C. W. Kensche. Fatigue of composites for wind turbines. *International Journal of fatigue,* 28:1363-1374, 2006.

[11] D. Mamalis, T. Flanagan and C. Ó Brádaigh. Effect of fibre straightness and sizing in carbon fibre reinforced powder epoxy composites. *Composites Part A: Applied Science and Manufacturing,* 110:93-105, 2018.

[12] Q. Wu, Y. Gu, S. Wang, X. Wang and Z. Zhang. Reaction of carbon fiber sizing and its influence on the interphase region of composites. *Journal of Applied Polymer Science,* 4197: 1-8, 2015.

[13] R. L. Zhang, Y. D. Huang, N. Li, L. Liu and D. Su. Effect of the concentration of the sizing agent on the carbon fiber surface and interface properties of its composites. *Journal of Applied Polymer Science,* 125:425-432, 2012.

[14] J. Maguire, K. Nayak and C. Ó Brádaigh. Characterization of epoxy powders for processing thick-section composite structures. *Materials and Design,* 139:112-121, 2018.

[15] X. Ramis, A. Cadenato, J. M. Morancho, J. M. Salla. Curing of a thermosetting powder coating by means of DMTA, TMA and DSC. *Journal of Polymer,* 44:2067-2079, 2003.

[16] S. Schmidt, T. Mahrholz, A. Kuhn and P. Wierach. Powder binders used for the manufacturing of wind turbine rotor blades. Part 1: Characterization of resin-binder interaction and preform properties. *Journal of Polymer Composites,* 708-717, 2018.

[17] R. Harshe. A review on advanced out-of-autoclave composites processing. *Journal of the Indian Institute of Science,* 95:3, 2015.

[18] C. Ó Brádaigh, S. Grant, J. Jury, D. Naylor, J. Shanks and T. Stratford, *Wave Energy Scotland Materials Landscaping Study,* hie.co.uk, 2016.

[19] J. Maguire, A. Doyle and C. Ó Brádaigh. Process modelling of thick-section tidal turbine blades using low-cost fibre reinforced polymers. *Proceedings of the 12th European Wave and Tidal Energy Conference, Cork, Ireland,* August 27-31 2017.

[20] J. Gao, Z. An and H. Kou. Fatigue life prediction of wind turbine rotor blade composites considering the combined effects of stress amplitude and mean stress. *Journal of Risk and Reliability,* 0:1-9, 2018.

[21] Y. Ma, Y. Yang, T. Sugahara and H. Hamada. A study on the failure behavior and mechanical properties of unidirectional fibre reinforced thermosetting and thermoplastic composites. *Composites: Part B,* 99:162-172, 2016.

[22] C. Kong, J. Bang and Y. Sugiyama. Structural investigation of composite wind turbine blade considering various cased and fatigue life. *Energy,* 30:2101-2014, 2005.

[23] H. J. Sutherland. A summary of the fatigue properties of wind turbine materials. *Wind Energy,* 3:1-34, 2000 .

[24] D. Mamalis, T. Flanagan, A. Doyle and C. Ó Brádaigh. A carbon fibre reinforced powder epoxy manufacturing process for tidal turbine blades. *Proceedings of the 12th European Wave and Tidal Energy Conference, Cork, Ireland,* August 27-312017.

[25] X. Chen. Structural degradation of a large composite wind turbine blade in a full-scale fatigue test. *Proceedings of the 2nd International Symposium on the Multiscale Experimental Mechanics; Multiscale Fatigue,* Lyngby, Denmark, November 8-9 2017.

[26] P. Alam, D. Mamalis, C. Robert, A. D. Lafferty and C. Ó Brádaigh. Mechanical properties and damage analyses of fatigue loaded CFRP for tidal turbine applications. *Proceedings of the 12th European Wave and Tidal Energy Conference, Cork, Ireland,* August 27-31 2017.

[27] J. M. Maguire, N.D. Sharp, R.B. Pipes and C.M. Ó Brádaigh. Process Simulations for Manufacturing Thick-Section Parts with Low-Cost Fibre Reinforced Polymers. *Proceedings of SAMPE Europe Conference, Stuttgart, Germany,* November 14-16 2017.

[28] P. Alam, C. Robert and C.M. Ó Brádaigh. Tidal turbine blade composites- A review on the effects of hygrothermal aging on the properties of CFRP. *Composites: Part B*, 149: in press, 2018.